Identification of BBX proteins as rate-limiting co-factors of HY5.

Katharina Bursch[1], Gabriela Toledo-Ortiz[2], Marie Pireyre[3], Miriam Lohr[1], Cordula Braatz[1], Henrik Johansson[1]*

1. Institute of Biology/Applied Genetics, Dahlem Centre of Plant Sciences (DCPS), Freie Universität Berlin, Albrecht-Thaer-Weg 6. D-14195 Berlin, Germany.

2. Lancaster Environment Centre, Lancaster University, Lancaster LA1 4YQ, UK

3. Department of Botany and Plant Biology, Section of Biology, Faculty of Sciences, University of Geneva, 30 Quai E. Ansermet, 1211 Geneva 4, Switzerland

*E-mail a.h.johansson@fu-berlin.de

Abstract

As a source of both energy and environmental information, monitoring the incoming light is crucial for plants to optimize growth throughout development[1]. Concordantly, the light signalling pathways in plants are highly integrated with numerous other regulatory pathways[2,3]. One of these signal integrators is the bZIP transcription factor HY5 which holds a key role as a positive regulator of light signalling in plants[4,5]. Although HY5 is thought to act as a DNA-binding transcriptional regulator[6,7], the lack of any apparent transactivation domain[8] makes it unclear how HY5 is able to accomplish its many functions. Here, we describe the identification of three B-box containing proteins (BBX20, 21 and 22) as essential partners for HY5 dependent modulation of hypocotyl elongation, anthocyanin accumulation and transcriptional regulation. The *bbx202122* triple mutant mimics the phenotypes of *hy5* in the light and its ability to suppress the *cop1* mutant phenotype in darkness. Furthermore, 84% of genes that exhibit differential expression in *bbx202122* are also HY5 regulated, and we provide evidence that HY5 requires the B-box proteins for transcriptional regulation. Lastly, expression of a truncated dark-stable version of HY5 (HY5ΔN77) together with BBX21 mutated in its VP-motif, strongly promoted de-etiolation in dark grown seedlings evidencing the functional interdependence of these factors. Taken together, this work clarifies long standing questions regarding HY5 action and provides an example of how a master regulator might gain both specificity and dynamicity by the obligate dependence of co-factors.

Main text

Light perception by the cryptochromes, phytochromes and UVR8 in plants results in the inhibition of the COP1/SPA E3 ubiquitin ligase complex that generally targets positive regulators of photomorphogenesis for degradation[9,10]. Exposure to light consequently results in the accumulation of several COP1/SPA targets that ultimately promote de-etiolation. Consequently, mutants of *cop1* exhibit photomorphogenic development when grown in darkness[11]. Out of the several targets of COP1 mediated protein degradation, the bZIP transcription factor HY5 plays the most prominent role in light-induced photomorphogenesis as a modulator of hypocotyl elongation, anthocyanin and chlorophyll accumulation, in addition to integrating numerous external and internal signalling pathways[5,12]. Genetically, mutants of *hy5* are largely epistatic to weaker alleles of *cop1* in darkness[13], suggesting that accumulation of HY5 is partly causing the *constitutively photomorphogenic (cop)* phenotype. This supports a model where light inhibition of COP1 results in HY5 accumulation followed by activation of transcriptional cascades that promote de-etiolation and photomorphogenesis (Fig 1a). Accordingly, HY5 protein levels progressively accumulate with increasing light intensities and correlate with a gradually stronger photomorphogenic phenotype in seedlings[12].

43   Interestingly, early reports showed that overexpression of *HY5* does not result in the expected strong
44   photomorphogenic phenotypes[14]. In addition, *in-planta* expression of a dark stable HY5 construct
45   (*HY5ΔN77*) does not promote de-etiolation in darkness[14]. These observations together with the
46   apparent lack of a transactivation domain in the HY5 protein[8], prompted an expansion of the linear
47   COP1-HY5 model to include an unknown factor X, that is negatively regulated by COP1 and is both
48   required and rate-limiting for HY5 to function (Fig. 1a)[14,15]. The model predicts the properties of factor
49   X as being negatively regulated by COP1 and functionally dependent on HY5. Furthermore, the *x*
50   mutant would phenotypically mimic *hy5*, while overexpression should result in hyper-
51   photomorphogenic phenotypes expected (but not seen) by overexpression of *HY5* (Fig. 1a).

52   Like HY5, the B-box Zinc finger transcription factors BBX20, BBX21 and BBX22 have been described as
53   positive regulators of photomorphogenesis[16-18]. Overexpression of these factors results in seedlings
54   strongly hypersensitive to light, and all are negatively regulated by COP1 at a post-transcriptional
55   level[18-20]. In addition, these three factors directly interact with HY5 *in planta*, and HY5 appears to be
56   largely required for their function[17,21,22]. Thus, as these BBX proteins fulfil many of the predicted
57   properties of factor X, we hypothesised that these BBX proteins have a functional role in modulating
58   the transcriptional capacity of the master regulator HY5 (Fig. 1a).

59   To genetically test the hypothesis, we first evaluated the phenotype of a *bbx20-1* null mutant
60   generated by CRISPR/Cas9 editing (Extended Data Fig. 1a, b). The *bbx20-1* mutant displayed a long
61   hypocotyl phenotype that co-segregated with the genotype and which could be restored by
62   complementation using a genomic *BBX20* construct (Extended Data Fig. 1c-e). In contrast to the
63   supressed hypocotyl elongation observed in two transgenic lines overexpressing *GFP-BBX20* ~20- and
64   ~40-fold, the *bbx20-1* mutant showed a long hypocotyl phenotype in monochromatic red, blue and
65   far-red light (Extended Data Fig. 2a, b) to which *hy5* appeared largely epistatic (Extended Data Fig. 2c).
66   Furthermore, while the BBX20 overexpressing lines showed a small phenotype in darkness as
67   previously reported[18], the *bbx20-1* monogenic mutant behaved like WT (Extended Data Fig. 2b, c).
68   However, *bbx20-1* partially supressed the dark phenotype of *cop1* mutants, consistent with BBX20
69   being targeted by COP1 for degradation[18] (Extended Data Fig. 2d). To investigate redundancy, the
70   *bbx20-1* mutant was then crossed with *bbx21-1bbx22-1* to generate the *bbx202122* triple mutant.
71   Indeed, redundancy was evident as an incremental increase in hypocotyl length was observed for
72   single, double and triple mutants when grown in red light, while no significant differences was
73   observed in darkness (Fig. 1b). Furthermore, as postulated by the model, the *bbx202122* mutant
74   largely mimicked both the strong hypocotyl phenotype and reduced anthocyanin accumulation of *hy5*
75   and no additive phenotypes were observed in the *bbx202122hy5* mutant, consistent with the view that
76   these factors are operating in the same pathway (Fig. 1c, d).

77   To further test this hypothesis we investigated transcriptomic changes in the *bbx202122 vs WT* through
78   RNA-seq analysis of 4-day-old seedlings grown in monochromatic red light. GO analysis of the 142
79   differentially expressed genes (DEGs) in *bbx202122* (Supplementary Data 1) revealed biological
80   processes related to cell wall organization, hydrogen peroxide, flavonoids, UV-B, red light and auxin
81   (Fig. 1e), largely consistent with the observed phenotypes. Reassuringly, we found that 119 (~84%) of
82   *bbx202122* DEGs were also miss-regulated in the *hy5* mutant grown under the same conditions (Fig.
83   1f and Supplementary Data 1). In this overlap, all but one gene were co-regulated between the two
84   mutants whereas 64% were co-down regulated, indicating that HY5 and these B-box proteins primarily
85   act to promote transcription of common targets (Fig. 1g). Based on the three most highly enriched GO-
86   terms (Fig. 1e), we further analysed *XTH12/13/26, PRX7/26/44*, *MYB12*, *F3H* and *FLS1* by qPCR and
87   found that these genes were similarly down-regulated in both *bbx202122* and *hy5* compared to WT
88   (Fig. 1h-j). In addition, we observed comparable elevation of transcript abundance of *XTH18*, *PRX53*
89   and *IAA6* in *bbx202122* and *hy5* (Extended Data Fig. 3), verifying the RNA-seq results. Importantly, no

additional miss-regulation was observed in the *bbx202122hy5* mutant (Fig. 1h-j, Extended Data Fig. 3), consistent with a model where BBX20-22 and HY5 work largely interdependently to regulate these transcripts. Overall, comparing the phenotypic and transcriptional analyses with the model predictions, the B-box proteins match the requirements for factor X (Fig. 1a), as key modulators of HY5 function.
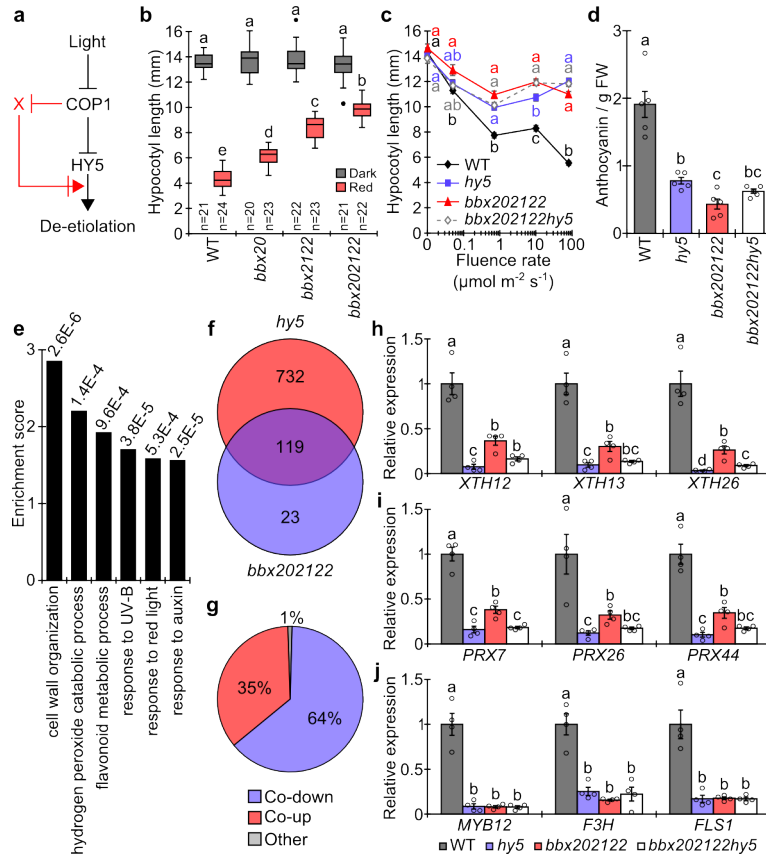
**Figure 1. BBX20-22 and HY5 are interdependently promoting photomorphogenesis. a)** Model of the linear COP1-HY5 pathway (black) and the HY5-X module extension (red) regulating de-etiolation. Adapted from Ang *et al.* 1998. **b)** Hypocotyl measurements of 5-day-old seedlings grown in constant darkness or 80 µmol m^{-2} s^{-1} red light. Box plots represent medians and interquartile ranges with whiskers extending to the largest/smallest value and outliers are shown as dots. **c)** Hypocotyl measurements of indicated mutant seedlings grown for 5 days at different fluence rates of red light. Data represents means ± SE. n= 27, 34, 33, 31, 39 for WT, 28, 28, 34, 34, 31 for *hy5*, 26, 27, 30, 34, 32 for *bbx202122*, 27, 31, 33, 30, 29 for *bbx202122hy5* from left to right. Statistical tests were performed within each treatment. **d)** Anthocyanin measurements of indicated seedlings grown as in (b). Data represents means ± SE. n=5 independent biological replicates. **e)** Gene Ontology analysis of *bbx202122* DEGs, from 4-day-old seedlings grown in 80 µmol m^{-2} s^{-1} of red light, as determined by DAVID 6.8. **f)** Venn diagram showing overlap between *bbx202122* and *hy5* DEGs. **g)** Pie-chart indicating percentages of co-regulation from the *bbx202122* and *hy5* overlap in (f). **h-j)** Analysis of *XTH12*, *XTH13*, *XTH26* (h) *PRX7*, *PRX26*, *PRX44* (i) *MYB12*, *F3H* and *FLS1* (j) transcript abundance relative to the *GADPH* and *TFIID* reference genes in 4-day-old seedlings grown in 80 µmol m^{-2} s^{-1} of red light. n=4 independent biological replicates. Data represents means and error bars represent SE. Different letters denote statistical significant differences (p<0.05) as determined by one-way (c-d, h-j) or two-way (b) ANOVA followed by Tukey's Post Hoc test. Open circles indicate single biological measurements.

Both BBX20 and BBX21 have previously been shown to promote the transcript levels of *HY5*[20,22]. In our conditions, *bbx202122* showed a ~35% reduction in *HY5* transcript levels which was ~4 and ~10 fold over-compensated in two independent transgenic *bbx202122* lines overexpressing *HY5* (Extended Data Fig. 4a). Further corroborating the functional interdependence of HY5 and BBX20-22, these two lines were not phenotypically different from *bbx202122* when grown in red light or darkness (Extended Data Fig. 4b), rejecting the possibility that the observed *bbx202122* mutant phenotype is due to a reduction of *HY5* levels.

119 To investigate the functional interdependence of HY5 and the B-box proteins at the post-
120 transcriptional level, we performed transient expression assays using *bbx202122hy5hyh* mutant
121 protoplasts. Two reporter constructs were created (*pMYB12^{-588}::GUS* and *pF3H^{-398}::GUS*) containing the
122 promoter sequence known to be directly bound and regulated by HY5[23-25] (Fig. 2a, b). Consistent with
123 the requirement of a cofactor to activate transcription, HY5 had little to no effect on the expression of
124 the *pMYB12^{-588}* and *pF3H^{-398}* reporters when expressed alone (Fig. 2c-e). However, when co-expressed
125 together with BBX20-22, HY5 strongly activated the *pMYB12^{-588}::GUS* reporter, while co-expression of
126 BBX21-22 (but not BBX20) resulted in strong activation of *pF3H^{-398}::GUS* (Fig. 2c-e). Quantification of
127 HY5-YFP in single protoplasts expressed alone or together with CFP-BBX21 revealed no difference in
128 HY5 accumulation (Extended Data Fig. 4c). Taken together, this suggests that HY5 is dependent on the
129 B-Box proteins for transcriptional regulation. Interestingly, yeast-two-hybrid (Y2H) experiments
130 probing the interaction between HY5 and BBX21-22 has previously been performed without the
131 addition of an activation domain to the BBX bait[17,21]. Including BBX20, we show that all of these B-box
132 proteins have the capability to activate transcription when bound to HY5 in a heterologous yeast
133 system (Extended Data Fig. 5a). Consistently, we identified a predicted transactivation domain (TAD)
134 in both BBX20 and BBX21 (Extended Data Fig. 5b) and found that a 33aa fragment of BBX21 containing
135 the predicted 9aaTAD was sufficient to strongly activate transcription in yeast (Extended Data Fig. 5c,
136 d). To investigate the possible importance of this TAD, we first generated a full length BBX21$_{mTAD}$
137 construct in which 5 amino acids within the TAD were exchanged to alanine (Extended Data Fig. 5b).
138 While, BBX21$_{mTAD}$ retained its ability to interact with HY5 in yeast (Extended Data Fig. 5e), the combined
139 ability of HY5 and BBX21$_{mTAD}$ to activate the *pF3H^{-398}::GUS* reporter in protoplasts was severely
140 reduced, suggesting a functional role of the predicted TAD (Fig. 2f). Reassuringly, fusing the
141 transactivation domain of VP16 to the C-terminal of BBX21$_{mTAD}$ restored the ability to activate
142 transcription together with HY5 (Fig. 2f). Taken together, these results are supporting a mechanism
143 where HY5 binds to promoter regions and the B-box proteins associate with DNA-bound HY5 to allow
144 transcriptional regulation. To further test this hypothesis, we performed ChIP-qPCR experiments for
145 BBX20 and BBX21, where the GFP-tagged BBX proteins were immunoprecipitated in a WT or in a *hy5*
146 mutant background. Targeting the *MYB12* and *F3H* promoter regions previously shown to be
147 immunoprecipitated by HY5[25] (Fig. 2a, b), we observed BBX specific enrichment for both promoters in
148 the WT genetic background (Fig. 2g, h and Extended Data Fig. 6a-d). However, this enrichment was
149 reduced in the *hy5* mutant, suggesting that HY5 is partly required for BBX-DNA association (Fig. 2g, h
150 and Extended Data Fig. 6a-d). Interestingly, although some DNA association was still present in the *hy5*
151 mutant, the promotion of *MYB12* and *F3H* transcript levels observed in *35S::GFP-BBX20* was
152 completely dependent on HY5 (Fig. 2i), similar to the short hypocotyl phenotype and high anthocyanin
153 accumulation seen in this line (Fig. 2j-k). To investigate if the BBX proteins are required for HY5 to
154 associate with promoter regions, we performed ChIP-qPCR experiments using a native HY5 antibody
155 on WT, *hy5*, *bbx202122* and *35S::GFP-BBX20* seedling samples. Interestingly, this analysis revealed
156 decreased and increased HY5 binding to the *MYB12* promoter in *bbx202122* and *35S::GFP-BBX20*,
157 respectively (Extended Data Fig. 7a). However, while immunoblotting using the HY5 antibody did not
158 detect any specific signal in our red light conditions, the reduced and increased *HY5* transcript levels
159 in *bbx202122* and *35S::GFP-BBX20* are consistent with the B-box proteins affecting HY5 abundance
160 rather than HY5-DNA association (Extended Data Fig. 7b).

161
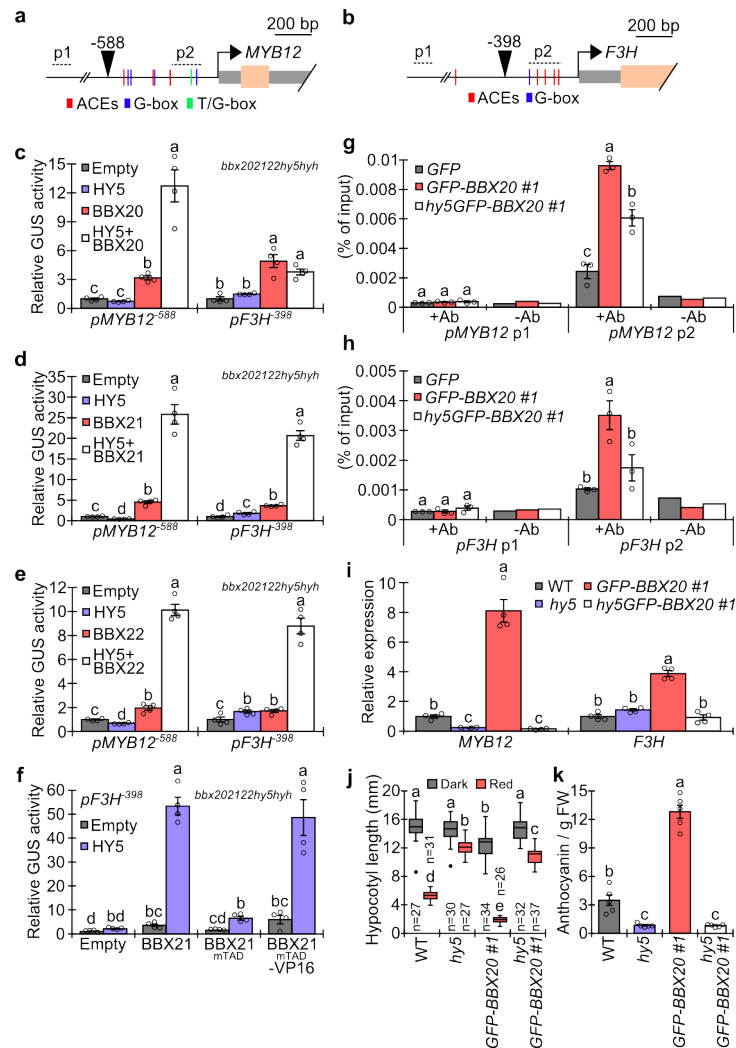
Figure 2. HY5 requires BBX proteins for transcriptional regulation. a-b) Schematic of the *MYB12* and *F3H* promoter region. Gray indicates 5' UTR and introns, beige indicates exon, respectively. Dotted line indicates sequence amplified for ChIP-qPCR where the non-binding control (p1) is located 1216-1493 and 742-945 bp upstream of the *MYB12* and *F3H* transcriptional start site, respectively. Arrowhead indicates the first base of the *pMYB12^-588^::GUS* and *pF3H^-398^::GUS* reporter constructs relative to the transcriptional start site. **c-e)** Transient expression of BBX20, BBX21, BBX22 and HY5 in *Arabidopsis bbx202122hy5hyh* protoplasts using the *pMYB12^-588^::GUS* or *pF3H^-398^::GUS* reporter constructs. n=4 biological replicates. **f)** Transient expression of HY5, BBX21, BBX21$_{mTAD}$ and BBX21$_{mTAD}$-VP16 in *Arabidopsis bbx202122hy5hyh* protoplasts using the *pF3H^-398^::GUS* reporter construct. n=4 biological replicates. **g-h)** Chromatin immunoprecipitation using no antibody (-Ab) or an anti-GFP antibody (+Ab) on samples harvested from 4-day-old *35S::GFP*, *35S::GFP-BBX20 #1* and *hy5 35S::GFP-BBX20 #1* transgenic seedlings grown in 80 μmol m^{-2} s^{-1} of red light. p1 and p2 denotes primer pairs amplifying a non-binding control region and HY5 binding region, respectively. n=3 biological replicates for +Ab samples and a single sample for -Ab. **i)** Transcript analysis of *MYB12* and *F3H* shown as relative to the reference genes *GADPH* and *TFIID* in 4-day-old seedlings grown in 80 μmol m^{-2} s^{-1} of red light. n=4 biological replicates. **j)** Hypocotyl measurements of 5-day-old seedlings grown in darkness or 80 μmol m^{-2} s^{-1} of red light. Box plots represent medians and interquartile ranges with whiskers extending to the largest/smallest value and outliers are shown as dots. **k)** Anthocyanin measurements of seedlings grown as in (j). n=5 biological replicates. Bar graphs represent means ± SE and different letters represent statistical significant differences (p<0.05) as determined by one-way (c-i, k) or two-way (j) ANOVA followed by Tukey's Post Hoc test. Open circles indicate single biological measurements.

In darkness, our working model (Fig. 1a) suggests that the *cop1* mutant seedling phenotype results from the accumulation of both HY5 and factor X and predicts that *bbx202122* should be equally epistatic to *cop1* mutant alleles as *hy5*. To test this prediction, we generated the *cop1-4bbx202122* mutant and observed a suppression of the short *cop1-4* hypocotyl phenotype similar to *cop1-4hy5* (Fig. 3a). Likewise, using the temperature sensitive *cop1-6* background[26], no difference in hypocotyl elongation was observed between *bbx202122* and *hy5* (Fig. 3b, c). In line with the proposed interdependency of these factors, *cop1-4bbx202122hy5* did not show any significant additional

187 elongation phenotype compared to the respective double and quadruple mutants (Fig. 3a).
188 Intriguingly, additional elevation of BBX20 protein levels in the *cop1-4* mutant by overexpression
189 resulted in a *fusca*-like phenotype (Extended Data Fig. 8a). This phenotype was also dependent on the
190 presence of HY5 (Extended Data Fig. 8a), suggesting that the BBX-HY5 module is functional at multiple
191 developmental stages and might contribute to the reported *fusca* phenotype of seedling-lethal *cop1*
192 null mutants[27]. Collectively, these results suggest that accumulation of HY5 together with the three B-
193 box proteins under study, are largely responsible for the *cop1* phenotype. In addition, the reported
194 lack of a *cop* phenotype in seedlings expressing the dark stable HY5ΔN77 construct[14] may result from
195 COP1 dependent degradation of the B-box proteins[18-20]. To test this hypothesis, we first identified a
196 potential VP-motif in BBX21, showing similarity to the VP-motifs of HY5, BBX24 and BBX25, which are
197 required for their interaction with COP1 (Extended Data Fig. 8b)[28,29]. We mutated the Val-Pro pair to
198 Ala-Ala to create BBX21$_{VP-AA}$ and expressed this construct in Arabidopsis under the control of the 35S
199 promoter and fused with an N-terminal GFP. Consistent with increased stability in darkness, this
200 construct accumulated to a higher degree than GFP-BBX21 in the dark, although expressed to a lower
201 extent (Extended Data Fig. 8c, d). Next, we expressed BBX21$_{VP-AA}$ under the control of XVE in
202 *Arabidopsis*, allowing for transcriptional induction by the addition of 17-β-estradiol (Est) (Extended
203 Data Fig. 8e). The *XVE::BBX21$_{VP-AA}$* transgenic line was then crossed to *hy5 35S::HY5ΔN77* in addition to
204 the relevant controls, to analyse hypocotyl elongation in the F$_1$ generation when grown in darkness
205 with or without the addition of Est. In line with the proposed model, no phenotypes were observed
206 when only one side of the module was expressed (Fig. 3d, e). However, as predicted, co-expression of
207 BBX21$_{VP-AA}$ (induced by the addition of Est) and HY5ΔN77 resulted in a partly de-etiolated seedling,
208 resembling a *cop* seedling (Fig. 3d, e).

209 Transcript analysis of the four crosses grown on Est showed a ~70-90 and ~7-9 fold overexpression of
210 *HY5ΔN77* and *BBX21$_{VP-AA}$*, respectively (Extended Data Fig. 8f). Furthermore, analysis of *XTH12/13/26*,
211 *PRX7/26/44*, *MYB12*, *F3H* and *FLS1* revealed that BBX21$_{VP-AA}$ together with HY5ΔN77 strongly promotes
212 the accumulation of these transcripts in darkness, while little effect was observed when expressed
213 alone (Extended Data Fig. 8g-i). These results that mirror the transcriptional analysis of the
214 *bbx202122hy5* mutant (Fig. 1h-j), further support the required presence of B-box proteins for HY5's
215 capacity to act as a transcriptional regulator. As recently reported[15], in agreement with the model and
216 a mechanism where the BBX proteins provide transcriptional capability to HY5, seedlings harbouring a
217 *35S::VP16HY5ΔN77* construct exhibited phenotypes similar to the combined expression of *BBX21$_{VP-AA}$*
218 and *HY5ΔN77* when grown in darkness, suggesting that the requirement of BBX proteins for HY5 to
219 promote de-etiolation can be bypassed by the addition of a TAD (Fig. 3f and Extended Data Fig. 8j).

220
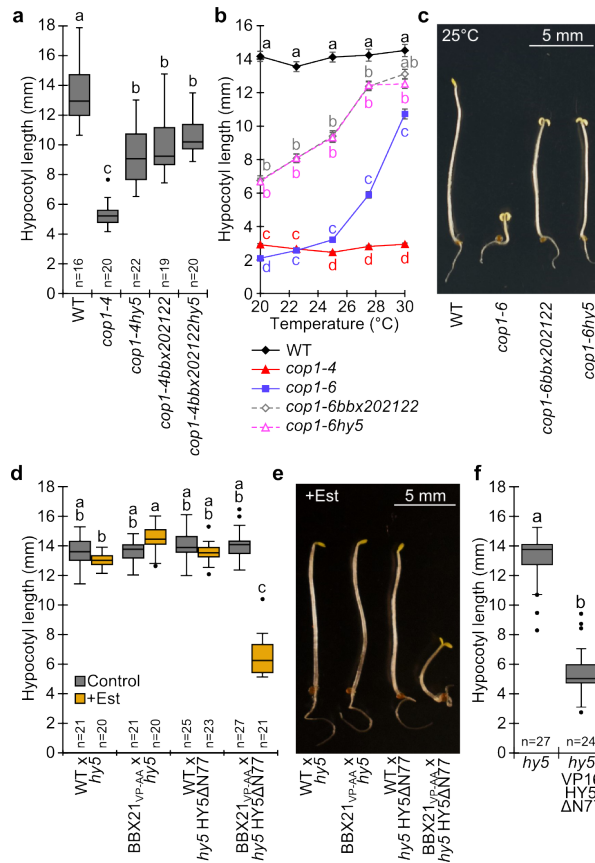
Figure 3. COP1 suppression of the HY5-BBX module inhibits de-etiolation in darkness. a) Hypocotyl measurements of 5-day-old seedlings grown in darkness. One-way ANOVA, Tukey's Post Hoc test. **b)** Hypocotyl measurements of seedlings grown for 1 day at 20°C and 4 additional days at the indicated temperature in darkness. Data represents means ± SE. n= 30, 31, 31, 32, 28 for WT, 30, 34, 35, 35, 34 for *cop1-4*, 29, 33, 35, 35, 34 for *cop1-6*, 34, 36, 33, 35, 28 for *cop1-6bbx202122*, 34, 36, 36, 36, 25 for *cop1-6hy5* from left to right and statistical tests were performed within each temperature treatment. **c)** Representative seedlings from (b) grown at 25 °C. **d)** Hypocotyl measurements of 5-day-old F_1 crosses between WT, *hy5*, *XVE::BBX21_{VP-AA}* and *hy5 35S::HA-HY5ΔN77* grown with 20 μM of 17-β-estradiol (+Est) or 0.1% ethanol (v/v) (Control). **e)** Representative seedlings from (d) grown on Est. **f)** Hypocotyl measurements of 5-day-old dark grown T_1 *hy5* mutant seedlings transformed with *35S::VP16HY5ΔN77* and non-transformed *hy5* siblings. The pFAST-G02 vector used allowed for selection of primary transformed seeds in the T_1 generation. Different letters represent statistically significant differences (p<0.05) as determined by one-way (a, b) or two-way (d) ANOVA followed by Tukey's Post Hoc test or Mann-Whitney-U-Test (f). Box plots represent medians and interquartile ranges with whiskers extending to the largest/smallest value and outliers are shown as dots.

In summary, the presented genetic and molecular data strongly suggests that BBX20-22 are acting as essential co-factors of HY5, surprisingly compatible with a working model proposed over two decades ago postulating that HY5 requires additional co-factors to function[14]. In light of these results, the model explains the observation that HY5ΔN77 does not cause a COP phenotype when expressed in darkness and further illuminates the molecular network underlying the *cop1* phenotype. Although our data supports a role for these B-box proteins in HY5 dependent regulation of hypocotyl elongation and anthocyanin accumulation, the fact that *bbx202122* only affected around ~15% of *hy5*-regulated genes indicate the presence of additional co-factors (Fig. 1f). Hence, the ability of HY5 to specifically and dynamically modulate various responses throughout plant development might depend on the specific temporal and spatial regulation of its co-factors, as described for master regulators in other biological systems[30].

References

1   Sullivan, J. A. & Deng, X. W. From seed to seed: the role of photoreceptors in Arabidopsis development. *Developmental biology* **260**, 289-297 (2003).

2   Lau, O. S. & Deng, X. W. Plant hormone signaling lightens up: integrators of light and hormones. *Curr Opin Plant Biol* **13**, 571-577, doi:10.1016/j.pbi.2010.07.001 (2010).

3   Paik, I., Kathare, P. K., Kim, J. I. & Huq, E. Expanding Roles of PIFs in Signal Integration from Multiple Processes. *Mol Plant* **10**, 1035-1046, doi:10.1016/j.molp.2017.07.002 (2017).

4   Koornneef, M., Rolff, E. & Spruit, C. J. P. Genetic Control of Light-inhibited Hypocotyl Elongation in Arabidopsis thaliana (L.) Heynh. *Zeitschrift für Pflanzenphysiologie* **100**, 147-160, doi:https://doi.org/10.1016/S0044-328X(80)80208-X (1980).

5   Gangappa, S. N. & Botto, J. F. The Multifaceted Roles of HY5 in Plant Growth and Development. *Molecular plant* **9**, 1353-1365 (2016).

6   Chattopadhyay, S., Ang, L. H., Puente, P., Deng, X. W. & Wei, N. Arabidopsis bZIP protein HY5 directly interacts with light-responsive promoters in mediating light control of gene expression. *Plant Cell* **10**, 673-683, doi:DOI 10.1105/tpc.10.5.673 (1998).

7   Zhang, H. *et al.* Genome-wide mapping of the HY5-mediated gene networks in Arabidopsis that involve both transcriptional and post-transcriptional regulation. *The Plant journal : for cell and molecular biology* **65**, 346-358 (2011).

8   Oyama, T., Shimura, Y. & Okada, K. The Arabidopsis HY5 gene encodes a bZIP protein that regulates stimulus-induced development of root and hypocotyl. *Genes Dev* **11**, 2983-2995, doi:10.1101/gad.11.22.2983 (1997).

9   Galvao, V. C. & Fankhauser, C. Sensing the light environment in plants: photoreceptors and early signaling steps. *Current opinion in neurobiology* **34**, 46-53 (2015).

10   Podolec, R. & Ulm, R. Photoreceptor-mediated regulation of the COP1/SPA E3 ubiquitin ligase. *Curr Opin Plant Biol* **45**, 18-25, doi:10.1016/j.pbi.2018.04.018 (2018).

11   Deng, X. W. *et al.* COP1, an Arabidopsis regulatory gene, encodes a protein with both a zinc-binding motif and a G beta homologous domain. *Cell* **71**, 791-801 (1992).

12   Osterlund, M. T., Hardtke, C. S., Wei, N. & Deng, X. W. Targeted destabilization of HY5 during light-regulated development of Arabidopsis. *Nature* **405**, 462-466 (2000).

13   Ang, L. H. & Deng, X. W. Regulatory hierarchy of photomorphogenic loci: allele-specific and light-dependent interaction between the HY5 and COP1 loci. *The Plant cell* **6**, 613-628 (1994).

14   Ang, L. H. *et al.* Molecular interaction between COP1 and HY5 defines a regulatory switch for light control of Arabidopsis development. *Molecular cell* **1**, 213-222 (1998).

15   Burko, Y. *et al.* Chimeric Activators and Repressors Define HY5 Activity and Reveal a Light-Regulated Feedback Mechanism. *The Plant Cell*, tpc.00772.02019, doi:10.1105/tpc.19.00772 (2020).

16   Chang, C. S. *et al.* LZF1, a HY5-regulated transcriptional factor, functions in Arabidopsis de-etiolation. *Plant J* **54**, 205-219, doi:10.1111/j.1365-313X.2008.03401.x (2008).

17   Datta, S., Hettiarachchi, C., Johansson, H. & Holm, M. SALT TOLERANCE HOMOLOG2, a B-box protein in Arabidopsis that activates transcription and positively regulates light-mediated development. *The Plant cell* **19**, 3242-3255 (2007).

18   Fan, X.-Y. *et al.* BZS1, a B-box protein, promotes photomorphogenesis downstream of both brassinosteroid and light signaling pathways. *Molecular plant* **5**, 591-600 (2012).

19   Chang, C.-S. J., Maloof, J. N. & Wu, S.-H. COP1-mediated degradation of BBX22/LZF1 optimizes seedling development in Arabidopsis. *Plant physiology* **156**, 228-239 (2011).

20   Xu, D. *et al.* BBX21, an Arabidopsis B-box protein, directly activates HY5 and is targeted by COP1 for 26S proteasome-mediated degradation. *Proceedings of the National Academy of Sciences of the United States of America* **113**, 7655-7660 (2016).

21   Datta, S. *et al.* LZF1/SALT TOLERANCE HOMOLOG3, an Arabidopsis B-box protein involved in light-dependent development and gene expression, undergoes COP1-mediated ubiquitination. *The Plant cell* **20**, 2324-2338 (2008).

297 22 Wei, C.-Q. *et al.* The Arabidopsis B-box protein BZS1/BBX20 interacts with HY5 and mediates
298   strigolactone regulation of photomorphogenesis. *Journal of genetics and genomics = Yi chuan*
299   *xue bao* **43**, 555-563 (2016).
300 23 Shin, J., Park, E. & Choi, G. PIF3 regulates anthocyanin biosynthesis in an HY5-dependent
301   manner with both factors directly binding anthocyanin biosynthetic gene promoters in
302   Arabidopsis. *Plant J* **49**, 981-994, doi:10.1111/j.1365-313X.2006.03021.x (2007).
303 24 Stracke, R. *et al.* The Arabidopsis bZIP transcription factor HY5 regulates expression of the
304   PFG1/MYB12 gene in response to light and ultraviolet-B radiation. *Plant Cell Environ* **33**, 88-
305   103, doi:10.1111/j.1365-3040.2009.02061.x (2010).
306 25 Hajdu, A. *et al.* ELONGATED HYPOCOTYL 5 mediates blue light signalling to the Arabidopsis
307   circadian clock. *Plant J* **96**, 1242-1254, doi:10.1111/tpj.14106 (2018).
308 26 Ma, L. *et al.* Genomic evidence for COP1 as a repressor of light-regulated gene expression and
309   development in Arabidopsis. *The Plant cell* **14**, 2383-2398 (2002).
310 27 Misera, S., Muller, A. J., Weiland-Heidecker, U. & Jurgens, G. The FUSCA genes of Arabidopsis:
311   negative regulators of light responses. *Mol Gen Genet* **244**, 242-252, doi:10.1007/bf00285451
312   (1994).
313 28 Holm, M., Hardtke, C. S., Gaudet, R. & Deng, X. W. Identification of a structural motif that
314   confers specific interaction with the WD40 repeat domain of Arabidopsis COP1. *The EMBO*
315   *journal* **20**, 118-127 (2001).
316 29 Lau, K., Podolec, R., Chappuis, R., Ulm, R. & Hothorn, M. Plant photoreceptors and their
317   signaling components compete for COP1 binding via VP peptide motifs. *EMBO J*, e102140,
318   doi:10.15252/embj.2019102140 (2019).
319 30 Spiegelman, B. M. & Heinrich, R. Biological control through regulated transcriptional
320   coactivators. *Cell* **119**, 157-167, doi:DOI 10.1016/j.cell.2004.09.037 (2004).
321 31 McNellis, T. W. *et al.* Genetic and molecular analysis of an allelic series of cop1 mutants
322   suggests functional roles for the multiple protein domains. *Plant Cell* **6**, 487-500,
323   doi:10.1105/tpc.6.4.487 (1994).
324 32 Toledo-Ortiz, G. *et al.* The HY5-PIF regulatory module coordinates light and temperature
325   control of photosynthetic gene transcription. *PLoS Genet* **10**, e1004416,
326   doi:10.1371/journal.pgen.1004416 (2014).
327 33 Fauser, F., Schiml, S. & Puchta, H. Both CRISPR/Cas-based nucleases and nickases can be used
328   efficiently for genome engineering in Arabidopsis thaliana. *Plant J* **79**, 348-359,
329   doi:10.1111/tpj.12554 (2014).
330 34 Karimi, M., Inze, D. & Depicker, A. GATEWAY vectors for Agrobacterium-mediated plant
331   transformation. *Trends Plant Sci* **7**, 193-195 (2002).
332 35 Shimada, T. L., Shimada, T. & Hara-Nishimura, I. A rapid and non-destructive screenable
333   marker, FAST, for identifying transformed seeds of Arabidopsis thaliana. *Plant J* **61**, 519-528,
334   doi:10.1111/j.1365-313X.2009.04060.x (2010).
335 36 Zuo, J., Niu, Q. W. & Chua, N. H. Technical advance: An estrogen receptor-based transactivator
336   XVE mediates highly inducible gene expression in transgenic plants. *Plant J* **24**, 265-273,
337   doi:10.1046/j.1365-313x.2000.00868.x (2000).
338 37 Nakagawa, T. *et al.* Development of series of gateway binary vectors, pGWBs, for realizing
339   efficient construction of fusion genes for plant transformation. *J Biosci Bioeng* **104**, 34-41,
340   doi:10.1263/jbb.104.34 (2007).
341 38 Job, N., Yadukrishnan, P., Bursch, K., Datta, S. & Johansson, H. Two B-Box Proteins Regulate
342   Photomorphogenesis by Oppositely Modulating HY5 through their Diverse C-Terminal
343   Domains. *Plant Physiol* **176**, 2963-2976, doi:10.1104/pp.17.00856 (2018).
344 39 Vandesompele, J. *et al.* Accurate normalization of real-time quantitative RT-PCR data by
345   geometric averaging of multiple internal control genes. *Genome biology* **3**, RESEARCH0034
346   (2002).
347 40 Cock, P. J., Fields, C. J., Goto, N., Heuer, M. L. & Rice, P. M. The Sanger FASTQ file format for
348   sequences with quality scores, and the Solexa/Illumina FASTQ variants. *Nucleic Acids Res* **38**,
349   1767-1771, doi:10.1093/nar/gkp1137 (2010).

350 41   Langmead, B. & Salzberg, S. L. Fast gapped-read alignment with Bowtie 2. *Nat Methods* **9**, 357-
351   359, doi:10.1038/nmeth.1923 (2012).
352 42   Li, B. & Dewey, C. N. RSEM: accurate transcript quantification from RNA-Seq data with or
353   without a reference genome. *BMC Bioinformatics* **12**, 323, doi:10.1186/1471-2105-12-323
354   (2011).
355 43   Love, M. I., Huber, W. & Anders, S. Moderated estimation of fold change and dispersion for
356   RNA-seq data with DESeq2. *Genome Biol* **15**, 550, doi:10.1186/s13059-014-0550-8 (2014).
357 44   Huang, D. W., Sherman, B. T. & Lempicki, R. A. Bioinformatics enrichment tools: paths toward
358   the comprehensive functional analysis of large gene lists. *Nucleic acids research* **37**, 1-13
359   (2009).
360 45   Huang, D. W., Sherman, B. T. & Lempicki, R. A. Systematic and integrative analysis of large gene
361   lists using DAVID bioinformatics resources. *Nature protocols* **4**, 44-57 (2009).
362 46   Fang, F. *et al.* A vector set for systematic metabolic engineering in Saccharomyces cerevisiae.
363   *Yeast* **28**, 123-136, doi:10.1002/yea.1824 (2011).
364 47   Piskacek, S. *et al.* Nine-amino-acid transactivation domain: Establishment and prediction
365   utilities. *Genomics* **89**, 756-768, doi:10.1016/j.ygeno.2007.02.003 (2007).
366 48   Sprenger-Haussels, M. & Weisshaar, B. Transactivation properties of parsley proline-rich bZIP
367   transcription factors. *Plant J* **22**, 1-8 (2000).
368 49   Kirby, J. & Kavanagh, T. A. NAN fusions: a synthetic sialidase reporter gene as a sensitive and
369   versatile partner for GUS. *Plant J* **32**, 391-400 (2002).
370 50   Yoo, S. D., Cho, Y. H. & Sheen, J. Arabidopsis mesophyll protoplasts: a versatile cell system for
371   transient gene expression analysis. *Nat Protoc* **2**, 1565-1572, doi:10.1038/nprot.2007.199
372   (2007).
373 51   Martin, G. *et al.* Circadian Waves of Transcriptional Repression Shape PIF-Regulated
374   Photoperiod-Responsive Growth in Arabidopsis. *Current Biology* **28**, 311-+,
375   doi:10.1016/j.cub.2017.12.021 (2018).
376 52   Binkert, M. *et al.* UV-B-responsive association of the Arabidopsis bZIP transcription factor
377   ELONGATED HYPOCOTYL5 with target genes, including its own promoter. *Plant Cell* **26**, 4200-
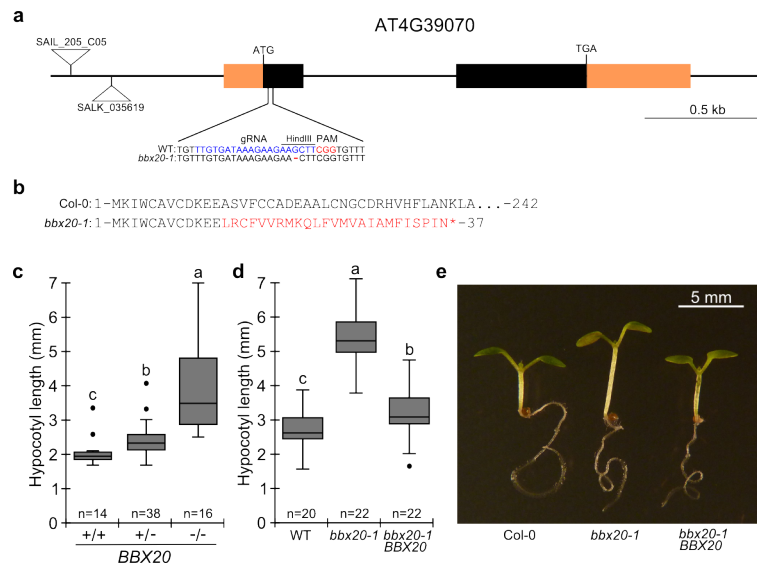378   4213, doi:10.1105/tpc.114.130716 (2014).
379 53   Oravecz, A. *et al.* CONSTITUTIVELY PHOTOMORPHOGENIC1 is required for the UV-B response
380   in Arabidopsis. *Plant Cell* **18**, 1975-1990, doi:10.1105/tpc.105.040097 (2006).
381 54   Wickham, H. ggplot2: Elegant Graphics for Data Analysis. *Use R*, 1-212, doi:10.1007/978-0-387-
382   98141-3 (2009).

383

384

385

Extended Data Figures

Extended Data Figure 1. Creation and validation of the *bbx20-1* mutant. a) Schematic representation of the *BBX20* locus indicating two available T-DNA insertion lines and the sequence targeted by CRISPR/Cas9. Orange areas indicate 5' and 3' UTR while black areas indicate the two exons of *BBX20*. Blue and red text indicate the gRNA and PAM sequence, respectively, used for CRISPR/Cas9 induced mutagenesis of *BBX20*. The recovered *bbx20-1* mutant harboured a 1-bp deletion 4-bp upstream of the PAM sequence, resulting in the loss of a HindIII recognition sequence available in the WT. **b)** Expected amino acid sequence of the *bbx20-1* mutant caused by the 1-bp frameshift. Frameshifted amino acids are labelled in red and the asterisk indicates an early stop-codon. **c)** Hypocotyl measurements of 68 5-day-old seedlings from a *bbx20-1* heterozygote parental plant grown in 100 μmol m^{-2} s^{-1} of red light. After measurements of the individual hypocotyls, PCR based genotyping revealed 14 WT, 38 heterozygote and 16 *bbx20-1* homozygote seedlings allowing for grouping each measurement into the three genotypes. **d)** Hypocotyl measurements of Col-0, *bbx20-1* and T$_1$ *bbx20-1* seedlings complemented with a genomic *BBX20* construct, utilizing the pFAST vector system for identification of transgenic seeds, grown as in (c). **e)** Photo of representative seedlings from (d). Box plots represent medians and interquartile ranges with whiskers extending to the largest/smallest value and outliers are shown as dots. Different letters represent statistical significant differences (p<0.05) as determined by one-way ANOVA followed by Tukey's Post Hoc test.

406
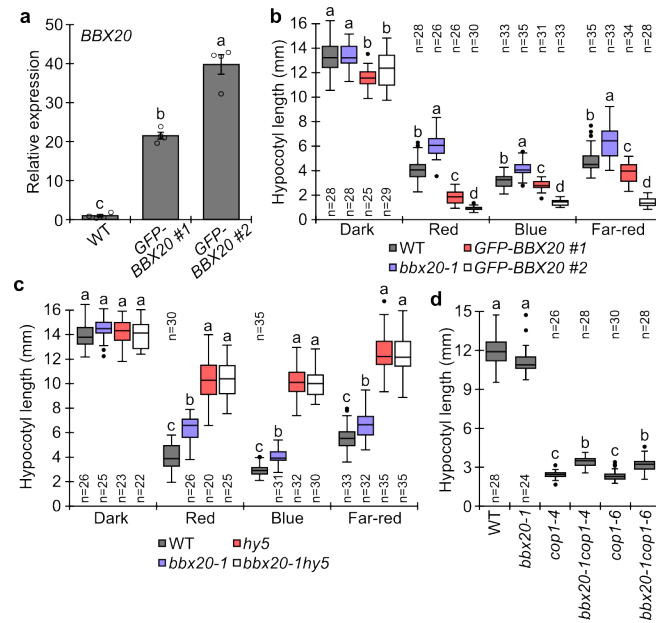
Extended Data Figure 2. BBX20 acts upstream of HY5 and downstream of COP1. a) *BBX20* transcript levels relative to the reference genes *ACT2* and *EF1A* in 4-day-old WT and *35S::GFP-BBX20* transgenic seedlings grown in 75 µmol m^{-2} s^{-1} of constant white light. n=4 biological replicates indicated by open circles. Data represents means ± SE. **b-c)** Hypocotyl measurements of 5-day-old seedlings grown in darkness, monochromatic red (80 µmol m^{-2} s^{-1}), blue (14 µmol m^{-2} s^{-1}) and far-red (1 µmol m^{-2} s^{-1}) light. **d)** Hypocotyl measurements of 5-day-old seedlings grown in darkness. Box plots represent medians and interquartile ranges with whiskers extending to the largest/smallest value and outliers are shown as dots. Different letters represent statistical significant differences (p<0.05) as determined by one-way ANOVA followed by Tukey's Post Hoc test.

414

415
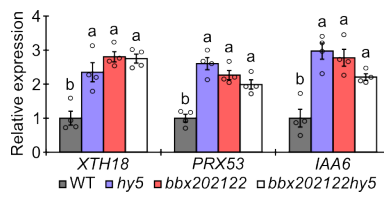
416

417

418

419

420

421

Extended Data Figure 3. Transcript analysis of genes inhibited by BBX20-22 and HY5. Analysis of *XTH18*, *PRX53* and *IAA6* transcript abundance relative to the *GADPH* and *TFIID* reference genes in 4-day-old seedlings grown in 80 μmol m^{-2} s^{-1} of red light. Data represents means ± SE. n=4 independent biological replicates. Different letters denote statistical significant differences (p<0.05) as determined by one-way ANOVA followed by Tukey's Post Hoc test. Open circles indicate single biological measurements.

427

428

429

430
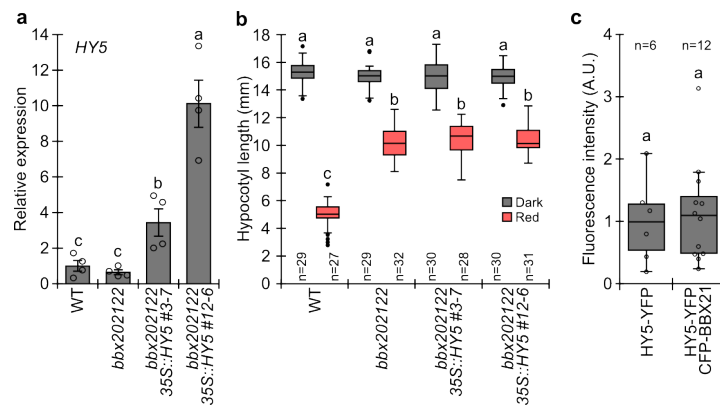
Extended Data Figure 4. The *bbx202122* phenotype is not due to reduced *HY5* transcript abundance. a) Transcript levels of *HY5* relative to *GADPH* and *TFIID* in 4-day-old seedlings grown in 80 µmol m^{-2} s^{-1} of red light. n=4 biological replicates indicated by open circles. Data represents means ± SE. Different letters represent statistical significant differences (p<0.05) as determined by one-way ANOVA followed by Tukey's Post Hoc test. **b)** Hypocotyl measurements of 5-day old seedlings grown as in (a) or constant darkness. Different letters represent statistical significant differences (p<0.05) as determined by two-way ANOVA followed by Tukey's Post Hoc test. **c)** Quantification of fluorescence intensity of YFP in the nuclei of *bbx202122hy5hyh* protoplasts transiently expressing HY5-YFP with or without CFP-BBX21. Different letters represent statistical significant differences (p<0.05) as determined by Student's t-test. Box plots represent medians and interquartile ranges with whiskers extending to the largest/smallest value and outliers are shown as dots.

440

441

442

443

444
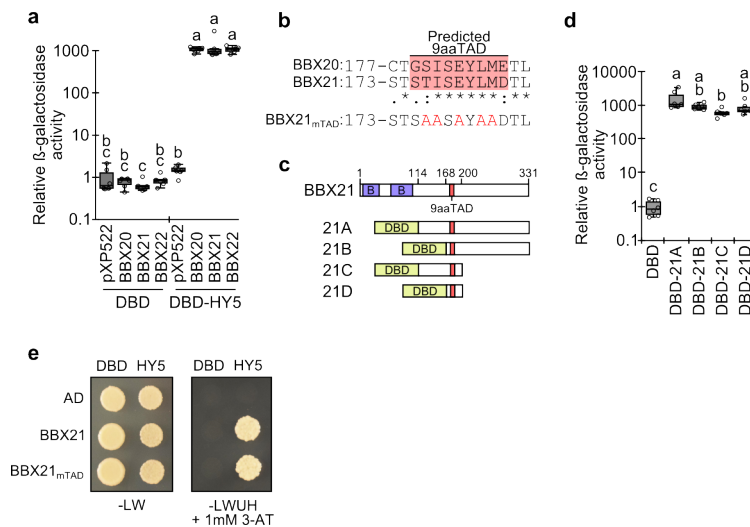
445

446

447

448

449

450

451

Extended Data Figure 5. A predicted 9aaTAD of BBX21 promotes transcription in yeast. a) Liquid yeast two-hybrid β-galactosidase assay using DBD-HY5 as bait and BBX20, BBX21 or BBX22 as prey not fused to an additional activation domain. Box plots represent medians and interquartile ranges with whiskers extending to the largest/smallest value and outliers are shown as dots. n=6. **b)** Alignment of predicted TAD region of BBX20 and BBX21 using Clustal Omega (1.2.4). BBX21mTAD shows the sequence after the introduction of 5 alanine residues **c)** Graphical representation of four truncated BBX21 constructs, 21A-21D, all containing the predicted 9aaTAD region. B and DBD represent B-box domain and DNA-binding domain, respectively. **d)** Measurements of auto activation of 21A, 21B, 21C and 21D fragments in yeast. n=6. **e)** Yeast two-hybrid assay using HY5 as bait and BBX21 or BBX21mTAD as prey. –LW and –LWUH indicate media lacking either Leu, Trp or Leu, Trp, Ura, His, respectively. 3-AT represents the addition of 3-amino-1, 2,4-triazol to the growth medium. The experiment was repeated with similar results using two independent sets of primary transformants. Single measurements are shown as open circles and statistical groups are indicated by letters as determined by one-way ANOVA followed by Tukey's Post Hoc test.

463
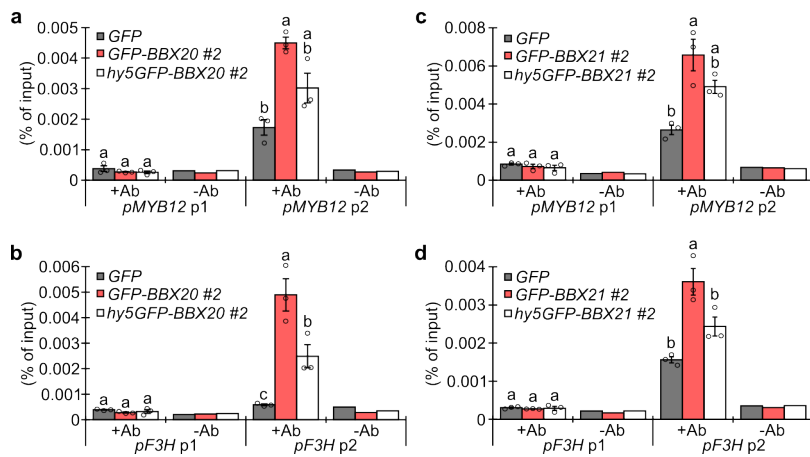
**Extended Data Figure 6. BBX20 and BBX21 associates with DNA dependent on HY5 in *Arabidopsis*. a-d)** Chromatin immunoprecipitation using no antibody (-Ab) or an anti-GFP antibody (+Ab) on samples harvested from 4-day-old *35S::GFP*, *35S::GFP-BBX20 #2* and *hy5 35S::GFP-BBX20 #2* (a, b) or *35S::GFP*, *35S::GFP-BBX21 #2* and *hy5 35S::GFP-BBX21 #2* (c, d) transgenic seedlings grown in 80 μmol m^{-2} s^{-1} of red light. p1 and p2 denotes primer pairs amplifying a non-binding control region and HY5 binding region, respectively. n=3 biological replicates for +Ab samples and a single sample for -Ab). Data represents means ± SE. Single measurements are shown as open circles and statistical groups are indicated by letters as determined by one-way ANOVA followed by Tukey's Post Hoc test.

477

478

479

480

481
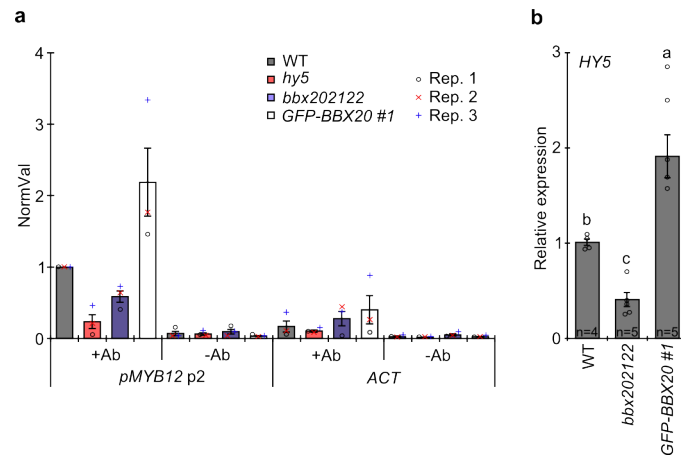
482

Extended Data Figure 7. HY5 binding to the *MYB12* promoter in *bbx202122* and *35S::GFP-BBX20 #1* correlate with *HY5* transcript levels. a) Chromatin immunoprecipitation using no antibody (-Ab) or an anti-HY5 antibody (+Ab) on samples harvested from 4-day-old WT, *hy5*, *bbx202122* and *35S::GFP-BBX20 #1* seedlings grown in 80 µmol m^{-2} s^{-1} of red light. p2 denotes primer pairs amplifying a HY5 binding region of the *MYB12* promoter as shown in Fig. 2a and *ACT* is used as negative control. n=3 independent biological replicates and each replicate was normalized to WT pMYB12 p2 +AB. Data represents means ± SE. Single measurements from each biological repeat is indicated by an open circle, cross and plus sign, respectively. **b)** Measurements of *HY5* transcript levels relative to *PP2A* in 4-day-old seedlings grown in 80 µmol m^{-2} s^{-1} of red light. Biological replicates indicated by open circles. Data represents means ± SE. Different letters represent statistical significant differences (p<0.05) as determined by one-way ANOVA followed by Tukey's Post Hoc test.

492

495
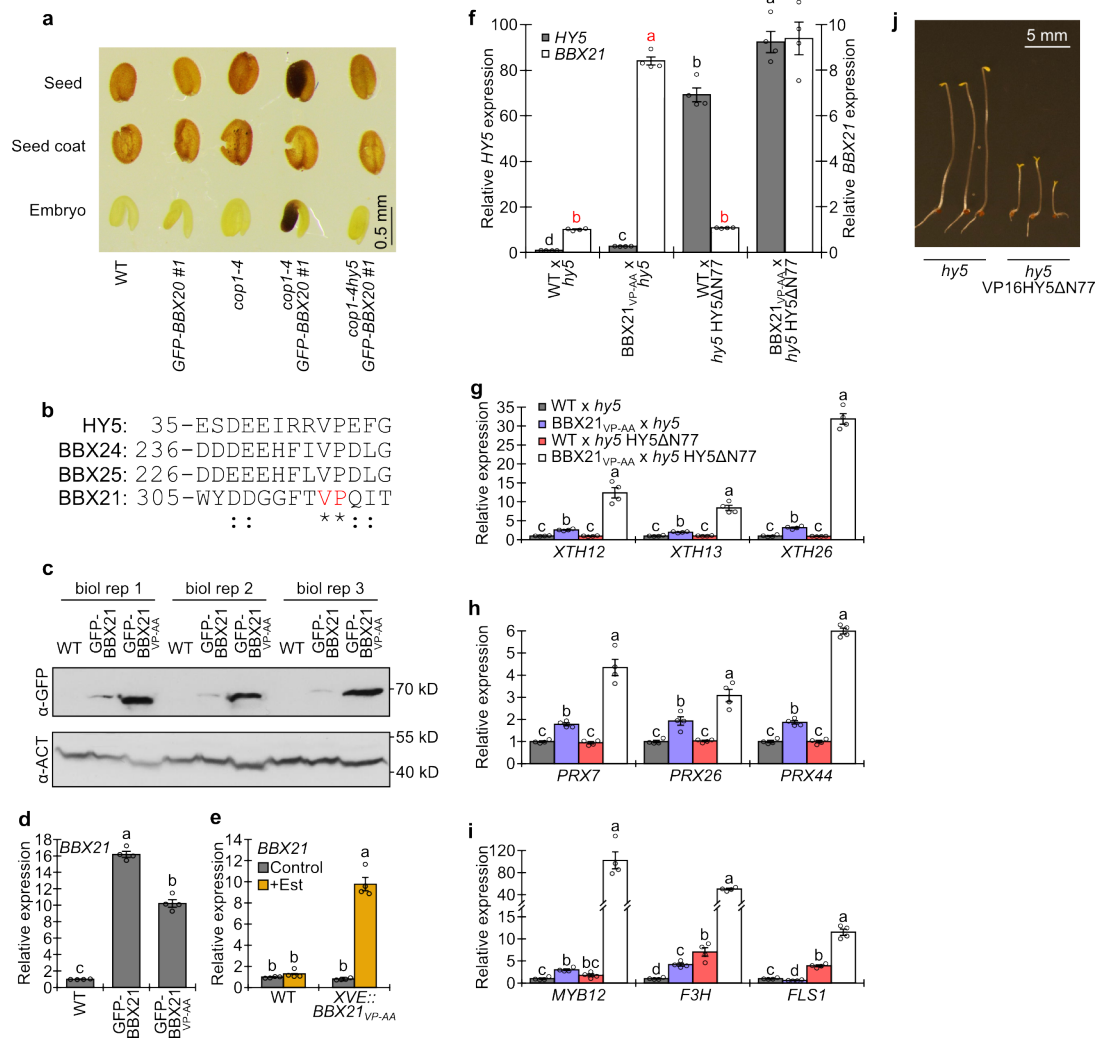
Extended Data Figure 8. Expression of BBX21$_{VP-AA}$ or a VP16 fusion is sufficient for HY5ΔN77 to promote photomorphogenesis. a) Photo of representative seeds, dissected embryos and seed coats of indicated genetic background. Similar observations were made over multiple generations. **b)** Alignment of VP-domain containing amino acids 35-47 of HY5, 236-248 of BBX24, 226-238 of BBX25 and 305-317 of BBX21, respectively, using Clustal Omega (1.2.4). The Val-Pro pair labelled red in BBX21 was modified to Ala-Ala to generate BBX21$_{VP-AA}$. **c)** Immunoblot analysis of total protein samples collected from transgenic seedlings expressing *GFP-BBX21* and *GFP-BBX21$_{VP-AA}$* driven by the 35S promoter, grown for 4 days in darkness. Anti-GFP and anti-ACT antibodies were used to detect the BBX proteins and the ACT loading control, respectively. 3 independent biological replicates are shown. **d)** *BBX21* transcript levels relative to the *GADPH* and *TFIID* reference genes in WT, *35S::GFP-BBX21* and *35S::GFP-BBX21$_{VP-AA}$* seedlings grown in darkness for 4 days. n=4. **e)** *BBX21* transcript levels relative to the *GADPH* and *TFIID* reference genes in WT and *XVE::BBX21$_{VP-AA}$* seedlings grown in darkness for 4 days with 20 µM of 17-β-estradiol (+Est) or 0.1% ethanol (v/v) (Control). n=4 biological replicates. **f)** Transcript levels of *HY5* and *BBX21* shown as relative to the *GADPH* and *TFIID* reference genes in the indicated crosses between WT, *hy5*, *XVE::BBX21$_{VP-AA}$* and *hy5 35S::HY5ΔN77* grown for 4 days in darkness on 20 µM of 17-β-estradiol. Black and red letters indicate significance for *HY5* and *BBX21* levels, respectively. n=4 biological replicates indicated by open circles. **g-i)** Analysis of *XTH12, XTH13, XTH26* (g) *PRX7, PRX26, PRX44* (h) *MYB12, F3H* and *FLS1* (i) transcript abundance relative to *GADPH* and *TFIID* in 4 day old seedlings grown as in (f). n=4 biological replicates indicated by open circles. Data represents means ± SE. Different letters represent statistical significant differences (p<0.05) as determined by one-way (d, f-h) or two-way (e) ANOVA followed by Tukey's Post Hoc test. **j)** Photo of representative 5-day-old dark grown *hy5* mutant seedlings or T$_1$ *hy5* mutant seedlings transformed with *35S::VP16HY5ΔN77*.

515

516

517
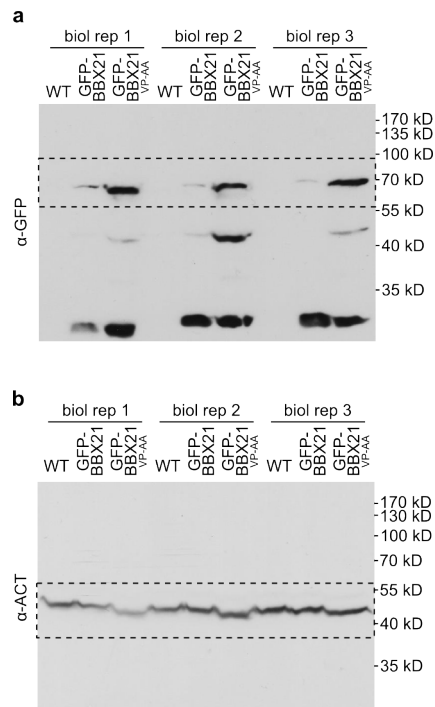
518

519

520

521 **Source Data Extended Data Fig. 8c. Scan of full immunoblots. a-b)** Immunoblots from Extended Data Fig. 8c using the anti-
522 GFP (a) or anti-ACT (b) antibody, respectively. Boxes represents cropped sections used for Extended Data Fig. 8c.

523

524

525 **Material and methods**

526

527

528 **Plant material and growth conditions**

529 All plant material used in this study originates from the *Arabidopsis* Col-0 accession. The *bbx21-1*,
530 *bbx22-1*, *hy5-215*, *hyh*, *cop1-4*, *cop1-6* have been described previously[8,17,21,31,32]. The *bbx20-1* point
531 mutation was created using a CRISPR/Cas9 system. A gRNA targeting the first exon (Extended Data Fig.
532 1a) was inserted in to the pEN-Chimera vector and shuttled to the pDE-CAS9 vector[33] using the
533 Gateway LR reaction. This vector was transformed into Col-0 and the mutants were identified by the
534 loss of the HindIII recognition site of a PCR product in T_2 plants that had lost the Cas9 cassette. Higher
535 order mutants were obtained by sequential crosses genotyped by PCR or by phenotype in the case of
536 *cop1-4* and *cop1-6*. To generate *35S::GFP-BBX20* lines, the full length *BBX20* CDS was amplified from
537 cDNA using the BBX20_LB_attB1 and BBX20_RBws_attB2 primers and inserted into the pDONR221
538 vector through the Gateway BP reaction. *BBX20* was then shuttled to the pB7WGF2 vector[34] to be
539 transformed into *Arabidopsis* by floral dip to generate GFP-BBX20 expressing lines under the control
540 of the 35S promoter.

541 For complementation analysis of the *bbx20-1* mutant a genomic fragment including 1 Kb promoter
542 region of *BBX20* was amplified from genomic DNA using the primers gBBX20_F and gBBX20_R. The PCR
543 fragment was then inserted into pDONR221 and shuttled into the pFAST-G01 vector[35]. The *bbx20-1*
544 mutant was then transformed with this construct, and hypocotyl lengths were measured in the T_1
545 generation utilizing the seed specific GFP selection marker.

546 To generate the BBX21$_{VP-AA}$ constructs, *BBX21* CDS was first amplified by PCR using the BBX21_LB_attB1
547 and BBX21_RP_VP-AA primers, followed by a consecutive PCR reaction using the BBX21_LB_attB1 and
548 BBX21_RBws_attB2 primers. This fragment was inserted into the pDONR221 vector and shuttled to
549 the pB7WGF2 and pMDC7[36] vectors. The BBX21$_{VP-AA}$ containing vectors were then transformed into
550 *Arabidopsis* Col-0 to generate *35S::GFP-BBX21$_{VP-AA}$* and *XVE::BBX21$_{VP-AA}$*.

551 The HY5_DN77_LB_attB1 and HY5RBws_attB2 primer were used to amplify the *HY5ΔN77* fragment
552 from cDNA, which was inserted into the pDONR221 vector and shuttled to the pGWB15[37] using
553 Gateway technology and later transformed into the *hy5-215* mutant to generate the *hy5 35S::*
554 *HY5ΔN77* transgenic lines. The pGWB15-HY5 vector has been described previously[38] and was
555 transformed into the *bbx202122* mutant to generate the *bbx202122 35S::HY5* lines. To generate *hy5*
556 *35S::VP16HY5ΔN77* the VP16 sequence was amplified from the pMDC7 plasmid using the VP16attB1
557 and VP16DN77_rev primer, and the *HY5ΔN77* fragment was amplified from cDNA using the
558 VP16DN77_fw and HY5RBws_attB2 primers. The two fragments were then fused by PCR using the
559 VP16attB1 and HY5RBws_attB2 primers to generate *VP16HY5ΔN77*. This construct was then inserted
560 into the pDONR221 vector and shuttled to the pFAST-G02 vector[35] which was transformed into the
561 *hy5-215* mutant using the floral dip method. All primers used for cloning are listed in Supplementary
562 Table 1.

563 Unless stated otherwise, surface sterilized seeds were sown on ½ MS-media, 0.05% (w/v) MES, pH 5.7,
564 1% agar (w/v), stratified for 3 days at 4°C in darkness followed by a 2-hour white light pulse (90 μmol
565 m^{-2} s^{-1}) and returned to darkness for 22 hours at 22°C before moved to the indicated experimental
566 conditions.

567

568 **Phenotypic analysis**

569 For hypocotyl measurements, 5 day old seedlings were flattened on the growth medium and
570 photographed before measurements were performed using the ImageJ software
571 (https://imagej.nih.gov/ij/). To measure anthocyanin levels, seedlings were collected, weighed and
572 frozen in liquid nitrogen before ground to a powder. 600 µl of extraction buffer (1% HCl (v/v) in
573 methanol) was added to the samples followed by an overnight incubation in darkness at 4°C. After the
574 addition of 650 µl chloroform and 200 µl dH$_2$O the samples were vortexed and centrifuged at 14000g
575 for 5 min. Anthocyanin levels were estimated by spectrophotometric measurement of the upper liquid
576 phase (A$_{530}$ and A$_{657}$) and calculated by the formula (A$_{530}$-0.33*A$_{657}$)/(tissue weight in gram). With the
577 exception of T$_1$ seedling analysis and segregation analysis (Fig. 3f and Extended Data Fig. 1c-d), all
578 experiments measuring hypocotyls lengths and anthocyanin levels were repeated three times with
579 similar results.

580

581 **Transcript analysis**

582 For total RNA isolation, samples were stratified for 2 days at 4 °C before given a 2-hour white light
583 pulse (~90 µmol m^{-2} s^{-1}). The samples were then kept in darkness for 22 hours before moved to the
584 experimental conditions or kept in darkness. After 3 additional days, the seedlings were harvested and
585 frozen in liquid nitrogen. Four biological replicates were analysed for each experiment. Total RNA was
586 extracted using RNeasy Plant Mini Kit (Qiagen) according to the manufacturer's instructions, including
587 an on-column DNAse treatment. cDNA was synthesised using Superscript III Reverse Transcriptase
588 (Invitrogen) with random N9 and dT25 primers following the manufacturer's instructions. The primer
589 pairs used for qPCR reactions are listed in Supplementary Table 1 and the qPCR was performed using
590 the CFX96 Real-Time System (Bio-Rad). *GADPH* and *TFIID* were used as reference genes unless stated
591 otherwise. Transcript levels relative to the control was calculated as previously described[39].

592 For RNA-sequencing, total RNA was extracted from Col-0, *hy5* and *bbx202122* seedlings that were
593 grown as above. Three independent biological replicates were sent to BGI (Hong Kong, China) for RNA
594 quality and integrity control, library synthesis, high-throughput sequencing and bioinformatic analysis.
595 In short, Agilent 2100 Bio analyzer was used to measure RNA concentration, RIN value, 28S/18S and
596 fragment length distribution. The mRNA was enriched by using oligo (dT) magnetic beads and double-
597 stranded cDNA was synthesized with random hexamer primers. After end repair the cDNA was 3'
598 adenylated and adaptors were ligated to the adenylated cDNA. The ligation products were purified
599 and enriched via PCR amplification, followed by denaturation and cyclization. The library products
600 were sequenced via the BGISEQ-500 platform. The raw sequencing reads (> 23 million) were filtered,
601 by removing reads with adaptors, reads with unknown bases and low quality reads to obtain clean
602 reads (approximately 23 million) which were stored in FASTQ format[40]. The clean reads were mapped
603 to TAIR10 using Bowtie2[41] and gene expression level was calculated with RSEM[42]. Differentially
604 expressed genes were identified with the Deseq2[43] method with the following criteria: fold-change ≥
605 2 and Bonferroni adjusted p-value ≤ 0.05. The RNA-seq data are deposited in NCBI's Gene Expression
606 Omnibus (GSE137147). Gene Ontology analysis was performed by DAVID 6.8[44,45] using
607 GOTERM_BP_FAT and medium classification stringency.

608

609 **Yeast assays**

610 For expression of BBX20-22 in yeast without the addition of an activation domain, the CDS of *BBX20-*
611 *22* were inserted into the pXP522 vector[46]. In short, BBX20, BBX21 and BBX22 CDS were amplified by

612   PCR using the primers XbaI_BBX20f and XhoI_BBX20r, XbaI_BBX21f and XhoI_BBX21r, XbaI_BBX22f
613   and XhoI_BBX22r, respectively, followed by XbaI and XhoI digestion and ligation into SpeI and XhoI
614   digested pXP522 vector. Construction of the bait vector pBTM116-HY5 has previously been
615   described[38]. For generating the BBX21 fragments, 21A-21D, with an N-terminal LexA-DBD fusion, the
616   primers BBX21DN133_attB1 and BBX21_RBws_attB2, BBX21-TAD_attB1 and BBX21_RBws_attB2,
617   BBX21DN133_attB1 and BBX21-TAD_attB2, BBX21-TAD_attB1 and BBX21-TAD_attB2 were used to
618   amplify 21A, 21B, 21C and 21D, respectively. The PCR fragments were used for a BP reaction into the
619   pDONR221 vector, followed by LR shuttling into the pBTM116 vector.

620   A 9aaTAD prediction tool[47] (https://www.med.muni.cz/9aaTAD) was used to identify the
621   transactivation domain in the BBX20 and BBX21 protein sequences. To generate the $BBX21_{mTAD}$
622   construct, *BBX21* CDS was first amplified by PCR using the BBX21_LB_attB1, mTAD_f and mTAD_r,
623   BBX21_RBws_attB2 primer pairs, followed by a consecutive PCR reaction using the BBX21_LB_attB1
624   and BBX21_RBws_attB2 primer. This fragment was inserted into the pDONR221 vector and shuttled
625   to pGAD42 vector to generate $AD-BBX21_{mTAD}$. Construction of the pGAD42-BBX21 vector has been
626   described previously[38].

627   β-galactosidase activity assay was performed following the protocol outlined in the Yeast Protocols
628   Handbook (Clonetech). In short, 6 individual primary transformed colonies were grown for each vector
629   combination in liquid –Leu –Trp medium. After protein extraction, β-galactosidase activity was
630   measured using o-Nitrophenyl-β-D-galactopyranosid (ONPG) as substrate. The activity was calculated
631   relative to the amount of cells (OD_{600}) and presented as relative to the empty vector control.
632   Alternatively, yeast was dropped on –Leu –Trp medium, or –Leu –Trp –Ura –His medium with the
633   addition of 1 mM 3-amino-1, 2,4-triazol (3-AT), and growth was recorded after 4 days at 30°C.

634

Immunoblotting

636   Etiolated seedlings grown for 4 days in darkness were flash frozen in liquid nitrogen and ground to a
637   fine powder. Total protein extraction, SDS-PAGE separation and transfer to PVDF membrane was
638   performed as previously described[38]. Anti-GFP (Takara Bio Clontech, #632380) and anti-ACT (Sigma,
639   #A0480) was used at a 1:2000 and 1:10000 dilutions, respectively, followed by the secondary anti-
640   mouse-HRP (Thermo Scientific, #31431) at a dilution of 1:10000. Complete scans of the membranes
641   are available as Source Data.

642

Protoplast assays

644   To generate $pDONR221-BBX21_{mTAD}-VP16$, the primer pair BBX21_LB_attB1, BBX21_r_C-VP16 was used
645   on $pDONR221-BBX21_{mTAD}$ template and BBX21_f_C-VP16, VP16_r_attB2 was used to amplify the VP16
646   domain from the pMDC7 vector. The two PCR fragments were fused by a consecutive PCR reaction
647   using the BBX21_LB_attB1, VP16_r_attB2 primer pair and the generated $BBX21_{mTAD}-VP16$ fragment
648   was inserted into the pDONR221 vector through the Gateway BP reaction. The full length *BBX22* CDS
649   was amplified from cDNA using the B22LB_attB1 and B22RBws_attB2 primers and inserted into the
650   pDONR221 vector. To express HY5, BBX20, BBX21, BBX22, $BBX21_{mTAD}$ and $BBX21_{mTAD}-VP16$ under the
651   35S promotor the full length CDS were shuttled from the respective pDONR221 vector (pDONR221-
652   HY5[38], pDONR221-BBX20, pDONR221-BBX21[38], pDONR221-BBX22, $pDONR221-BBX21_{mTAD}$, pDONR221-
653   $BBX21_{mTAD}-VP16$) to the pB2GW7 vector[34]. To generate the $pMYB12^{-588}::GUS$ reporter construct, a
654   fragment containing 700 bp upstream of the *MYB12* ATG start codon (588 bp upstream of the TSS) was
655   amplified from genomic DNA using the pMYB12_fwd_HindIII and pMYB12_rev_EcoRI primers. The

656 fragment was then digested with HindIII and EcoRI and ligated into the pBT10-GUS vector[48]. A 615 bp
657 fragment upstream of the *F3H* ATG start codon (398 bp upstream of the TSS) was amplified using the
658 pF3H_fwd_BamHI and pF3H_rev_EcoRI primers. After BamHI and EcoRI digestion, the fragment was
659 inserted into the pBT10-GUS vector to generate the *pF3H^-398^::GUS* reporter construct. All primers used
660 for the cloning are listed in Supplementary Table 1. As transformation control a plasmid containing the
661 synthetic NAN gene[49] under the control of the 35S promotor was used. For generating protoplasts,
662 seeds of the *hy5hyhbbx202122* mutant were sown on soil and stratified in darkness for 2 days at 4 °C.
663 The plants were then grown for 4 – 6 weeks in short day conditions (8 h light, 16 h dark) with 100 µmol
664 $m^{-2} s^{-1}$ white light at 21 °C. To isolate and transform the protoplasts, an adapted version of a previously
665 described protocol was used[50]. In short, leaves were cut with a scalpel and the protoplasts were
666 extracted by incubation in enzyme solution containing Cellulase "Onozuka" R-10 (Yakult Honsha Co.,
667 Ltd., Japan) and Macerozyme R-10 (Yakult Honsha Co., Ltd., Japan) (without vacuum) over night at 21
668 °C in the dark. The protoplasts were then filtered through a 60 µm nylon filter and washed twice with
669 W5 solution before resuspended in MMG solution to a concentration of 2 x 10^5 ml^{-1} and stored on ice
670 for 3 h - 24 h. 40000 protoplasts were then transformed with a mixture of expression vector, reporter
671 construct and transformation control by DNA-PEG-calcium-induced transfection. For each experiment,
672 the protoplasts were transformed with a reporter construct (*pMYB12^-588^::GUS* or *pF3H^-398^::GUS*), two
673 effector constructs (HY5, BBX20, BBX21, BBX22 or pB2GW7-empty) and the 35S::NAN control
674 construct. In total the protoplasts were transformed with 12.5 µg (for the BBX20 and BBX21$_{mTAD}$
675 experiments (Fig. 2c, f)) or 25 µg (for the BBX21 and BBX22 experiments) of total DNA, with a ratio of
676 2:1:1:1 (reporter:effector:effector:control). Each transformation was performed in four biological
677 replicates. After removing the PEG solution the protoplasts were incubated overnight (16 – 18 h) in
678 W1 solution with 70 µmol $m^{-2} s^{-1}$ red light. Samples were harvested in liquid nitrogen. GUS and NAN
679 activity was measured as described before[49] with 4-methylumbelliferyl ß-D-glucuronide (MUG) and 2'-
680 (4-methylumbelliferyl)-α-d-*N*-acetylneuraminic acid (MUN) as substrates. The results are given as GUS
681 activity relative to the NAN activity and all experiments were independently repeated three times.

682 For confocal laser scanning microscopy of Protoplasts, the full length CDS of *BBX21* was shuttled from
683 pDONR221-BBX21 into the pB7WGC2[34] vector via Gateway LR reaction. The full length CDS of *HY5* was
684 amplified without the stop codon using the HY5LB_attB1 and HY5RBns_attB2 primer pair and the
685 resulting fragment was inserted into the pDONR221 vector by the Gateway BP reaction and shuttled
686 by LR reaction into the pB7YWG2[34] vector. Protoplasts were generated and transformed with 5 µg of
687 pB7YWG2-HY5 and 5 µg of either pB7WGC2-BBX21 or pB7WGC2-empty as described above. The
688 protoplasts were incubated overnight (16 – 18 h) in 70 µmol $m^{-2} s^{-1}$ red light followed by analysis with
689 confocal laser scanning microscopy (Leica TCS SP5). Imaging was done with identical excitation
690 intensity and detection sensitivity. YFP was excited at 514 nm and fluorescence was detected at 520 –
691 580 nm. The fluorescence intensity of YFP was measured using the ImageJ software by defining the
692 nucleus as ROI and measuring the "integrated density" of this region. The experiment was performed
693 two times with similar results.

694

695 **Chromatin immunoprecipitation**

696 For experiments with BBX20 and BBX21, seedlings were sown on ½ MS-media, 0.05% (w/v) MES, pH
697 5.7, 1% agar (w/v) and stratified in darkness at 4 °C for 48 h before treated for 2 h with a white light
698 pulse (100 µmol $m^{-2} s^{-1}$). The seedlings were then kept in darkness at 20 °C for 22 h before moving
699 them to red light (80 µmol $m^{-2} s^{-1}$) for 72 h before harvesting. ChIP assays were conducted following
700 the protocol reported previously[51] with the following modifications. For immunoprecipitation, Anti-
701 GFP mAb-Magnetic Beads from MBL (Cat. #D153-11) or Protein A-Dynabeads (Invitrogen, Cat.
702 #10001D) were used overnight at 4°C for +Ab and -Ab controls, respectively. Three biological replicates

703 were performed for all the "+Ab" samples, and one for the "-Ab" control. RT-PCR was conducted
704 according to standard protocol in three technical replicates. Primers were designed to target a known
705 HY5 binding region "p2" (p2_MYB12_F, p2_MYB12_R and p2_F3H_F, p2_F3H_R) of the *MYB12* and
706 *F3H* promoter regions, or a sequence further upstream "p1" (p1_MYB12_F, p1_MYB12_R and
707 p1_F3H_F, p1_F3H_R) with no predicted HY5 binding, as negative control (Fig. 2a, b and
708 Supplementary Table 1). Calculations were based on the percent input method.

709 For experiments with HY5, ChIP was processed as described previously[52]. Shortly, 1 g of fresh material
710 was harvested and processed for crosslinking in PBS 3 % formaldehyde under vacuum for 2 x 10
711 minutes. The crosslinking reaction was quenched by adding Glycine to 0.2 M. After nuclei extraction
712 and sonication, the chromatin was immune-precipitated with antibodies against HY5[53]. qPCR data was
713 obtained using PowerUp SYBR Green Master Mix reagents and QuantStudio 5 real-time PCR system
714 (Applied Biosystem) with the p2_MYB12_F and p2_MYB12_R primer pair for the *MYB12* promoter
715 region and ip_ACT_F and ip_ACT_R for the *ACT2* negative control region. The qPCR data were analysed
716 according to the percentage of input method. To account for variation across the three experimental
717 replicates, IPs were normalized to the WT-IP for the *MYB12* p2 for each replicate.

718

719 **Data analysis**

720 Statistical analysis was performed using Prism7.03 (GraphPad Software, La Jolla, USA). The data was
721 tested for normality using Shapiro-Wilk normality test and equal variance using Brown-Forsythe test.
722 Log transformed or non-transformed data was then analysed by one-way or two-way ANOVA followed
723 by Tukey's Post Hoc test or two-tailed Mann-Whitney-U-Test as indicated. Statistically significant
724 groups ($p<0.05$) are indicated by different letters. Box-plots were generated with the ggplot2 (package
725 version 3.2.0)[54] in RStudio (version 1.1.453) (http://www.rstudio.com), where outliers are defined as
726 greater than 1.5*interquartile ranges.

727

733

734 **Author contributions**

735 H.J conceived, designed and directed the project. G.T.O and M.P performed ChIP-qPCR experiments
736 while M.L created *bbx20-1* and higher order mutants. K.B and C.B performed the protoplast assays
737 while H.J and K.B performed all other experiments. H.J and K.B analysed the data. H.J, K.B and G.T.O
738 wrote the manuscript and all authors revised the manuscript.

739

740 **Competing interests**

741 The authors declare no competing interests.

742

743 **Materials & Correspondence**

744 Correspondence and requests for materials used in this study should be addressed to
745 a.h.johansson@fu-berlin.de.

746

747 **Data Availability**

748 The RNA-seq data is deposited at NCBI's Gene Expression Omnibus under the accession number
749 GSE137147 at https://www.ncbi.nlm.nih.gov/geo/query/acc.cgi?acc=GSE137147. The source data for
750 Fig. 1b-d, h-j, Fig. 2c-k, Fig. 3a-b, d, f, and Extended Data Fig. 1c-d, 2a-d, 3, 4a-c, 5a, d, 6a-d, 7a-b, 8d-i
751 is provided with the manuscript.